Investigating the paraglacial and periglacial processes responsible for observed rockfall frequency at Abbott Ridge in the Northern Selkirk Mountains

A. Charbonneau, M. Kotack, G. Sedun

Department of Geography, University of Victoria, B.C., Canada.

Abstract

Rockfall dynamics in alpine areas are subject to static and dynamic factors that reduce slope stability, inducing differential failure in the landscape. In a deglaciated cirque, structural measurements coupled with a lichenometric survey indicate that rockfall frequency has changed over the past 250 years. Permafrost degradation in response to rising air temperatures is suggested as the dominant factor influencing variable failure frequencies; however, rockmass properties and paraglacial adjustment are also considered important for slope modification. Directions for further research at Abbott Ridge are discussed at length, both to further knowledge of rockslope stability and to inform protected areas management in Glacier National Park.

Keywords: Periglacial; Paraglacial; Rock mass; Slope Stability; Lichenometry; Rockfall frequency

1.1 Introduction

Cirques are common landscape features in alpine environments and develop through concentrated erosive activity on upper sides of mountain valleys. They are characterized by a sharp break in slope where a steep headwall meets a carved, circular depression of low-gradient and are confined downslope by a terminal moraine (Slaymaker, 2011). Forming in pre-existing depressions in the topography, cirque glaciers have historically occupied these concave arcs for tens to hundreds of thousands of years (Evans, 2006). These small glaciers are largely responsible for their shape through the removal of bedrock destabilized by freeze-thaw activity and subsequent transport through rotational flow to the toe. Cirques occupied by glaciers are

eroded both headward through mechanical weathering and joint-block exploitation and downward, by glacial abrasion and rotational flow (Olyphant, 1981; Evans, 2006). Over the past 100 years, researchers have debated the relative contribution of each erosive direction to the resultant morphology of cirques however, it is established that erosion must be greatest at the base of the headwall in order for the characteristic break of slope and low-gradient floor to result (Evans, 2006).

In the absence of glaciers, a different suite of dominant factors is responsible for failure and control the contemporary retreat rate and morphodynamics of the cirque (Matsuoka, 2008; McColl, 2012). Paraglacial processes are "non-glacial earth-surface processes, sediment accumulations, land systems and landscapes that are directly conditioned by both glaciation and deglaciation" (Ballantyne, 2002, p. 1938). Recent research has noted that consideration of paraglacial processes precedes a holistic understanding of landscape evolution in previously glaciated terrain (Ballantyne, 2002; Evans, 2006; Mercier, 2009; Slaymaker, 2011; McColl, 2012). Previous to this emphasis, changes to alpine landscapes were attributed mostly to periglacial processes such as freeze-thaw activity that occur in extremely cold regions (Ritter, Kochel, & Miller, 2002, p.359). In actuality, morphodynamics of alpine features such as cirques continue to be influenced by glacial activity despite their absence. As stated by Slaymaker (2011), ice-free cirques indicate modifications to the topographic legacy left behind by glacial periods, and provide a noteworthy location to investigate paraglacial landscape adjustment in concert with periglacial processes.

1.2 Research Objectives

In the Columbia Mountains, a widespread transition from glacier-dominated to periglacial-dominated processes is occurring as the climate continues to warm, promoting negative glacier mass-balances and upslope glacial retreat (Slaymaker, 2011). This is particularly obvious in cirques, as features previously covered are now subject to different weathering processes and mechanisms of transport. The research presented in this paper investigates the contemporary modification of an ice-free cirque located on the North-facing side of Abbott Ridge, within Glacier National Park, British Columbia. The aim of this research is to describe the dynamics of rockwall frequency during the late-Holocene. A review of the literature related to cirque evolution and rockfall activity will be used to interpret the results of a geomorphic assessment.

Structural geology and lichenometry will provide *in situ* descriptions of cirque modification over the last 300 years. General site observations will further describe the contemporary form of the Abbott Ridge cirque in the context of landscape response to paraglacial adjustment and periglacial processes.

2. Background information

Recent cirque modification occurs within the context of glacial activity, despite an observed transition towards periglacial processes, and is related to paraglacial landscape adjustment. Most cirques in the Canadian cordillera containing Holocene glacial deposits only appear to have late-Neoglacial legacies, such as unvegetated moraines, which indicate the major pulses of the 18th and 19th centuries. Otherwise known as the Little Ice Age, the late Holocene maximum extent ended at the beginning of the 20th century. From 1920-1950, ice retreat was rapid followed by a decline to contemporary retreat rates (Menounos, Clague, & Luckman, 2009). Glacier dynamics are indicative of climatic changes therefore their activity can be interpreted to determine periods of warming or cooling. In the Rocky Mountains, Watson & Luckman (2004) used dendrochronology for a 300-year climate reconstruction around the Peyto Glacier. Their results indicate that cumulative mass balance is negative after 1883, reflecting the increasing temperature trend in the region. The relationship between rockfall frequency and high mountain permafrost degradation has also been proposed as an indicator of rising mean annual air temperature (Deline, 2009; Ravanel & Deline, 2011). After an initial discussion of rockmass properties, factors related to paraglacial and periglacial rockslope stability during periods of climatic variability are reviewed.

2.1 Rock mass properties

Preconditioning factors are defined as “those which are static and inherent” (McColl, 2012, p.6), such as the rock-mass properties of lithology and rock structure, and are responsible for differential failure in glaciated landscapes. These properties exert the dominant control of stability and slope-failure patterns as the distribution of strengths and weaknesses within the face determines headwall response to imposed stresses (McColl, 2012). Failure within a rock occurs when a combination of stress, strain and temperature over time exceed a specific critical limit

(Edelbro, 2003). Tension, compression and shear forces induce stress and strain, and are the three primary mechanisms of rock failure (Figure 1).

Tensile failure results when tensional stress exceeds the critical value for a given substance or object, similar to stretching a rope until it snaps. The tensile or Young's modulus is by definition the ratio of uniaxial stress over the uniaxial strain. The tensile strength of a material is a measure of its stiffness. Relative typical values for some materials are: rubber at 15 MPa, quartzite at 10-30 MPa and granite at 7-25 MPa (Zhu, 2012). Comparing these values show that if the same tension is applied to these various materials, depending on their composition they would all fail at around the same time.

The ability of a rock to withstand compression is called the Bulk modulus. It is defined as the ratio of pressure increase relative to the change in volume. The compressive strength of a rock is the maximum force that can be applied before the rock mass fails. Relative values for various materials are: quartzite at 150-300 MPa, wood at 5 MPa and steel at 250 MPa (Zhu, 2012). These values imply that wood compresses relatively easily compared to the likes of steel and quartzite.

Shear force is described using the Shear modulus, and it is the ratio of shear stress to shear strain. The ability of a rock to withstand shear force is known as the shear strength. An example of this is spalling, when there is a significant shear stress under the surface. This is commonly caused by the absorption and subsequent freezing of water within a rock. The water expands upon freezing inducing a shear stress in all directions. Relative typical values of shear strength are: wood at 10 MPa, steel at 230 MPa, quartzite at 20-60 MPa and soft clay at 40 KPa (Zhu, 2012). This implies that when a shear stress is applied, the clay would fail first, followed by wood, quartzite and then steel.

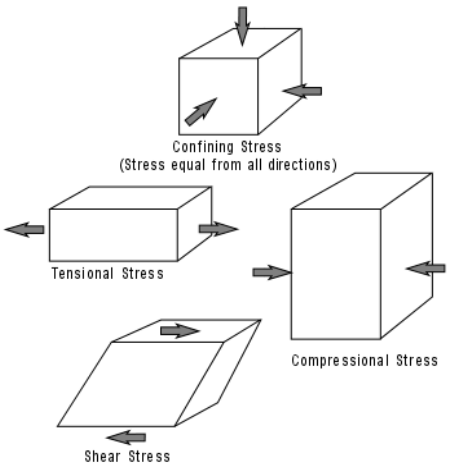

Figure 1. Differential stresses: actions and resultant deformation (Nelson, 2012).

The orientation and magnitude of all the stresses acting upon a body of rock have a direct impact on the orientation and scale of failure within the rock body; leading to a larger stress resulting in a greater fracture. To analyze this, Matsuoka & Sakai (1999), conducted window surveys to determine the joint spacing on a headwall. They found that "the size distribution of rock fall debris depends primarily on joint spacing" (Matsuoka & Sakai, 2009, p.325). While an understanding of these factors is essential for evaluating the drivers of contemporary cirque modification, the dynamic nature of paraglacial and periglacial processes provide a particularly interesting perspective from which to investigate rock fall frequency.

2.2 Paraglacial rock slope stability

Present-day headwall retreat in ice-less cirques is a result of numerous factors, static but also dynamic, encouraging instability. Paraglacial processes consist of preparatory factors that reduce slope stability over time without initiating movement (McColl, 2012). Glacial over-steepening, as is characteristic of cirques, results in steepened walls and deep valleys that increase the shear and self-weight stresses within slopes. These slopes are then susceptible to failure as glacial retreat removes support at the bottom of the headwall (McColl, 2012).

Failures of paraglacial origin also result from stress release (Cossart, Braucher, Fort, Bourlès, & Carcaillet, 2008). Glaciers can create new non-tectonic joint systems distinguishable by various features such as an increase in density towards the surface. These joints also have little to no filling material, and sometimes crosscut or terminate at tectonic fractures (McColl, 2012).

McColl (2012) bring specific attention to sheeting joints, which are most likely generated by high surface-parallel stresses, such as glacial mass on steep-slopes (See Figure 2. in Appendix A). With respect to cirques, glacial erosion produces steep headwalls and removes lateral confinement providing a local for stress-release and subsequent formation of sheeting joints. The resulting stress-release fractures may occur very soon after deglaciation or even during thinning or retreat; however, the timescale for their development following glacial stress-redistribution remains uncertain (McColl, 2012).

Non-tectonic joint systems significantly alter the stability and slope-failure pattern of the headwall, and are capable of both preconditioning and triggering paraglacial rock slope failure via stress unloading. Triggering factors change the slope from a 'marginally stable' to 'actively unstable' state (McColl, 2012). Undercutting from glacial debuttressing is an important factor influencing long-term slope failure (Holm, Bovis, & Jakob, 2004). Failure is triggered after sufficient glacial retreat or thinning at the toe when the buttressing ice is no longer supporting the wall (McColl, 2012). The paraglacial exhaustion conceptual model indicates that these processes of destabilization have a temporal window in which they operate. These factors exert a maximum influence on landscape response shortly after deglaciation, followed by a progressive decline in the frequency of rock slope failures. Although a useful tool for interpreting rock fall frequencies, the model takes no account of changing climatic influences (Ballantyne, 2002). Paraglacial processes have proven to dominate areas in the absence of periglacial processes (Ballantyne, 2002), however the response of freeze-thaw activity and permafrost to the climatic forces driving deglaciation are important to consider when apparent in the landscape (Kellerer-Pirklbauer, Lieb, Avian, & Carrivick, 2012).

2.2 Periglacial processes influencing rock slope stability

Periglacial processes are those controlled by intense frost action, are not reliant on permafrost and occur in locations free of snow cover for part of the year. Proximity to glaciers is not a necessary precursor to their function, thus periglacial processes are non-glacial (Ritter et al., 2002). The dominant cause of instability in periglacial landscapes is freeze-thaw activity. Where locations of weakness such as joints or bedding planes exist, mechanical weathering further reduces rockface stability through repetitive cycles of freeze-thaw activity. During rainfall or

snowmelt events water penetrates into the joints and induces frost heaving (vertical) and frost thrusting (horizontal) as the water freezes due to compressional forces from the water expanding by about 10% (Taber, 1930). Over time these compressional forces exert stress on the jointed rock face causing incremental movement away from the cliff face. After an unknown number of frost thrusting cycles the block has migrated far enough away from its original stable position that it topples to the ground below and is then deposited on the talus slope.

Climatic variability influences periglacial processes, providing another opportunity aside from glacial morphodynamics to determine landscape response. In high mountain areas, many steep rockwalls contain stabilizing permafrost where features such as ice-filled cracks are common. Warming permafrost leads to degradation that can cause slope instability, with convex topography such as ridges prone to faster and deeper thaw. Deep thawing during abnormally warm summers results in a thicker active layer, encouraging failure (Ravanel & Deline, 2011; Kellerer-Pirklbauer et al., 2012). In addition, permafrost degradation is strongly affected by percolating water in fractures (Gruber & Haeberli, 2007). With rising mean annual air temperatures over the 20th century, rockwall permafrost degradation has increased (Ravanel & Deline, 2011). Deline (2009) posits that this relationship could be responsible for the present rock fall rates, and earlier rates during warm periods of the Holocene.

The extent of permafrost in alpine areas is controlled by insolation and elevation, with the lowest elevation of permafrost around 2000m on very shaded slopes (Allen, Gruber & Owens, 2009). Allen et al. (2009) use potential radiation and elevation of a study site to classify it as mostly permafrost, marginal permafrost or mostly not permafrost (Figure 2 in Appendix A). Some marginal occurrences of alpine permafrost probably still reflect maximum Holocene cooling during the Little Ice Age, which culminated in the 19th century (Etzelmuller et al., 2001). The recently observed increase in rock fall frequency in the European Alps and Northern British Columbia has been attributed to the thinning and retreat of glaciers, permafrost degradation, and increased precipitation (Gruber & Haeberli, 2007; Geertsema, Clague, Schwab, & Evans, 2006).

3. STUDY SITE

3.1 Orogeny of the Selkirks and formation of Abbott Ridge

The Abbott Ridge Cirque is composed of Late Proterozoic meta-sammites (quartzite) with inter-bedded pelites (phyllite). Abbott Ridge is part of the Northern Selkirk Mountains belonging to the Columbia Mountain Range. The Columbia Mountains resulted from the opening of the Mid-Atlantic Ridge, after the break of Pangea around 210 million years ago. The formation of the Mid-Atlantic Ridge triggered the North American plate's movement westward to the subducting ancient oceanic plates. Occurring at the same time is the deposition of geosynclinal sediments off the coast of North America. Around 200 Ma the islands of the Intermontane terrane approached from the southwest and being less dense than North America, the Intermontane terrane accreted onto the North American Plate (Colpron, Warren & Price, 1998). This accretion forced the geosynclinal sediments up onto the North American plate. The extreme compressional force travelled as as series of waves from the accretion causing the geosynclinal sediments to form Western Canada's first mountain range: the Columbia Mountain Range (consisting of the Caribou, Selkirk, Purcell and the Monashee sub ranges). Between about 175-120 Ma, as the accretion compression wave continued to propagate toward the east it created a thrust fault creating the Rocky Mountains. The Insular Terrane then accreted at about 85 Ma causing another compression wave to propagate eastward forming the Calgary foothills amongst other features.

The rocks of the Abbot Ridge cirque are primarily composed of bedded phyllitic and feldspathic quartzite (metamorphosed sandstone that can retain the original bedding structure). The original sandstone was deposited among the other geosynclinal sediments and due to the accretion of the Intermontane Terrane was exposed to heating and pressure, fusing the sandstone grains with the cement. The creation of Abbott Ridge is the result of the geosynclinal sediments buckling under the compressional stress wave. Abbott Ridge is just one of many crests located along the Cheops fault, explaining the steepness of the end wall vertical fracture plane illustrated in Figure 5.

3.2 Geomorphic characteristics of Abbott Ridge and the cirque

The elevation of Abbott Ridge at the cirque study site is 2300m and indicates the height of the headwall (51 d 14’59’’N, 117 d 30’27” W). At the base of the steep, glacially carved headwall, a Neoglacial moraine confines a small glacier. Downslope of the moraine, a talus slope has developed that extends to a depression on the floor of the cirque. Towards the valley on the other side of the depression, a moraine-like feature delimits the extent of the Abbott Ridge cirque (Figure 2). On the lateral sides of the Abbott Ridge cirque, a treeline is apparent (Holm et al., 2004). Above the treeline, the slope is vegetated and contains the trail system; below, unvegetated blocky talus dominates the slope as shown in Figures 4 and 5. Annual winter air temperatures from 1870-2012 have risen by 1.5˚ Celsius, apparent from climate models for the Rogers Pass area (Figure 3).

The talus contained within the cirque is highly angular indicating the material has undergone passive transport and endured minor weathering after its release from the rockwall (Harrison, Anderson, & Patel, 2006). The Columbia Mountains are classified as temperate interior alpine mountains with a lower limit of periglacial around 2000m (French & Slaymaker, 1993). Based on the elevation and North-facing orientation of the Abbott Ridge headwall, the study site falls within the zone of marginal permafrost; the site is ~2000m and North facing with low potential radiation (Allen et al., 2009). Based on the angularity and dimensions of the boulders, and the scale of the feature, the talus deposit in the Abbott Ridge cirque bears similarity to ‘blockfields’. The culmination of frost heaving and thrusting constructs this periglacial feature (Worsley, 2007). The saxicolous crustose lichen *Rhizocarpon geographicum* is well-established on the talus features, encrustings the planar surfaces of the quartzite boulders.

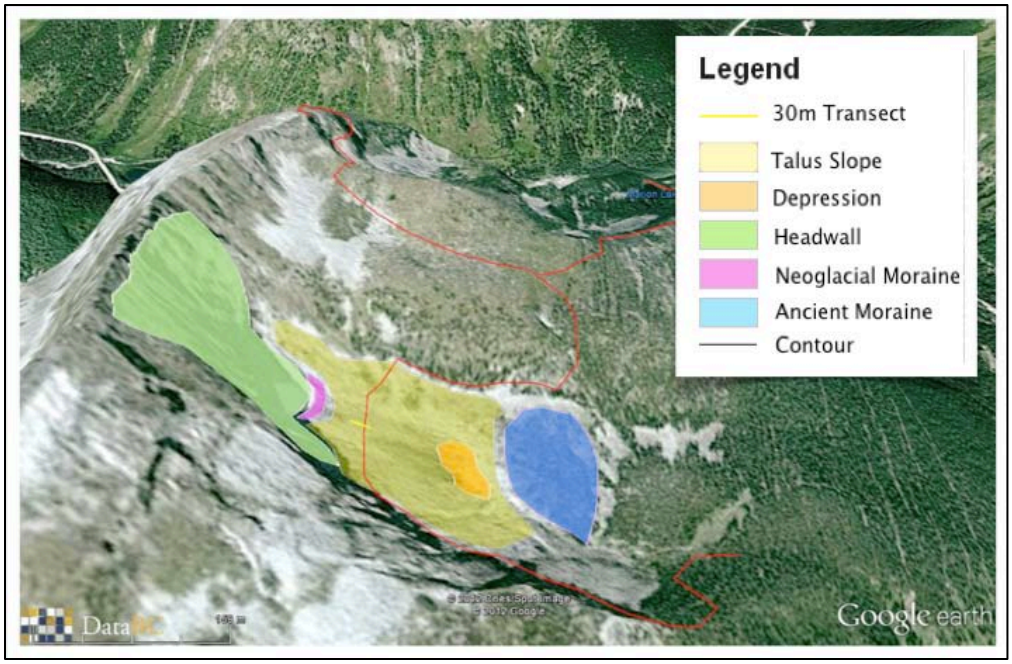

Figure 2. Geomorphic map of the Abbott Ridge study site, with major features described in the legend (Google Inc, 2012)

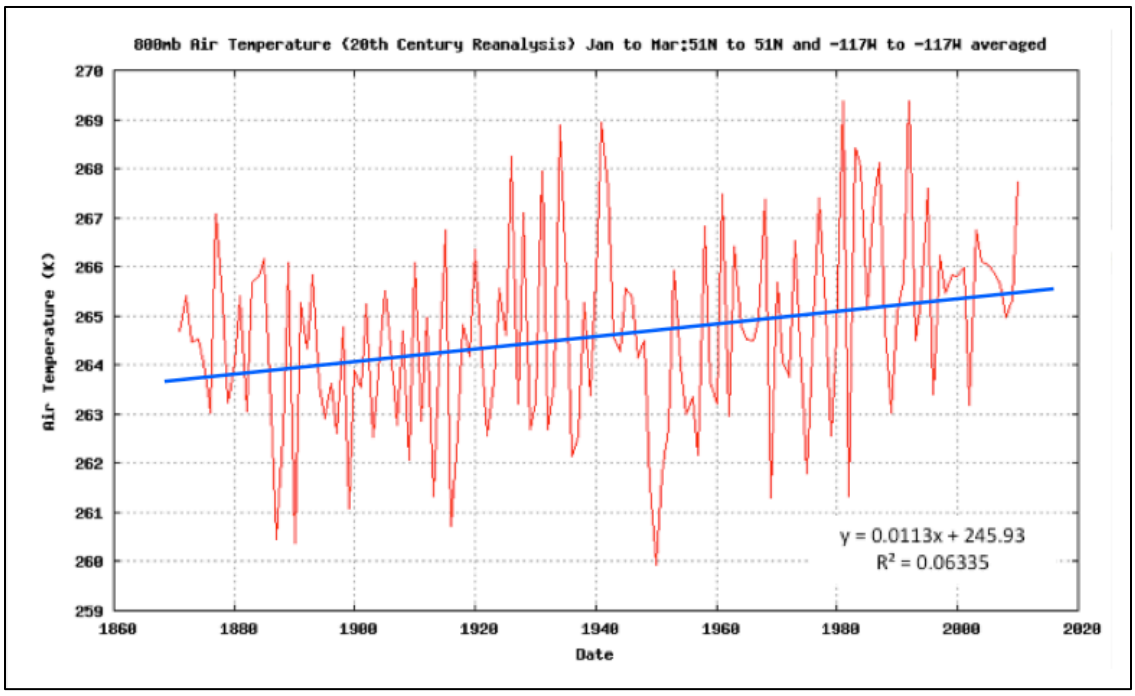

Figure 3. 20th Century Reanalysis V2 data for Rogers Pass provided by the NOAA/OAR/ESRL PSD, Boulder, Colorado, USA, from their Web site at http://www.esrl.noaa.gov/psd/ Source: Compo et al. (2011).

Figure 4. Looking down at the study site from on top of Abbott Ridge.
Source: Madison Kotack

Figure 5. Looking West towards the headwall of the cirque.
Source: Greg Sedun

4. METHODOLOGY

4.1 Structural measurements

Measurements of strike and dip angle of the failure planes in the field was done using a field compass that had inclination. The strike of a plane is the intersection between the plane and the horizontal surface. The dip angle of a plane is the inclination angle of the plane. Using the right hand rule, the thumb points in the direction of strike and the outstretched fingers represent the dipping plane. These measurements were then plotted using the Stereonet 7 application by Allmendinger, Cardozo & Fisher (2012) and are shown in Figure 6.

4.2 Lichenometric measurements

Initial observance of site conditions (i.e. boulder geology and distribution, elevation and tree sparsity) indicated that lichenometry was the most suitable dating technique for gauging rockfall activity. As the cirque was filled with lichen-encrusted boulders, a population approach that divided the site into 'sub-plots' -- individual boulders -- was used, whereby lichen thalli were measured within each sub-plot (Muller, 2006). This approach is also known as the 'frequency analysis approach,' and is popular among scientists as it can undergo more rigorous statistical testing (Muller, 2006; McCarroll, 1994). This approach is especially suitable to our research, as it allows dating of 'multi-aged surfaces', or sites which have experienced multiple rockfall events (Muller, 2006).

Actual data collection involved marking a 30-meter transect (using a meter tape) in the centre of the Abbott Ridge cirque: a location determined by analysis of site conditions (i.e. least disturbed tract with a multitude of boulders). Along this transect 30 boulders (sub-plots) were selected, and their location, size (small, medium or large), and aspect were recorded. On each boulder, the 3 largest lichen thalli were located and a digital caliper was used to measure (to the nearest tenth of a millimeter) the longest axis as well as the axis which ran perpendicular to it. Non-spherical lichen or closely merged lichen were excluded from sampling to prevent the potential measurement of an amalgamation of several lichen (McCarthy, 2003). The tops of boulders were also avoided, as they fulfilled a 'perch' role to local hoary marmots and pika, which may have fertilized lichen with their excrement and thus biased lichen growth (Parks

Canada, 2012). A sample size of three was decided on because it allowed statistical calculations such as the mean and median.

Once lichen data had been collected and prepared, a histogram was created to relate thallus size with frequency, and to reveal any potential size patterns (i.e. data peaks). This involved the development of 5-mm size classes of thalli, whereby the frequency of each thallus within a size class was recorded and graphed. Next, temporal patterns of lichen occurrence were sought through the use of a lichen growth curve. As substrate age within the Abbott Ridge cirque was unknown, it was assumed that McCarthy's (2003) *R. geographicum* growth curve for the proximal Illecillewaet Glacier would be highly similar. McCarthy integrated the lichen ecesis interval (<5 years) into the curve, so, upon removal of Illecillewaet data plots, our data was inserted. The largest thallus size within each subplot was interpolated along the curve, which produced approximate dates and temporal patterns of rock fall activity within the cirque.

5. RESULTS

5.1 Structural measurements

As shown below in Figures 6, 7 and 8, the rockwall consists of three fracture planes. The horizontal fracture plane is striking 328˚ with a dip of 40˚; the end vertical fracture plane with a strike/dip at 322/78˚; finally, the side vertical plane with a strike/dip of 231/84˚. The poles to each fracture plane are represented as points.

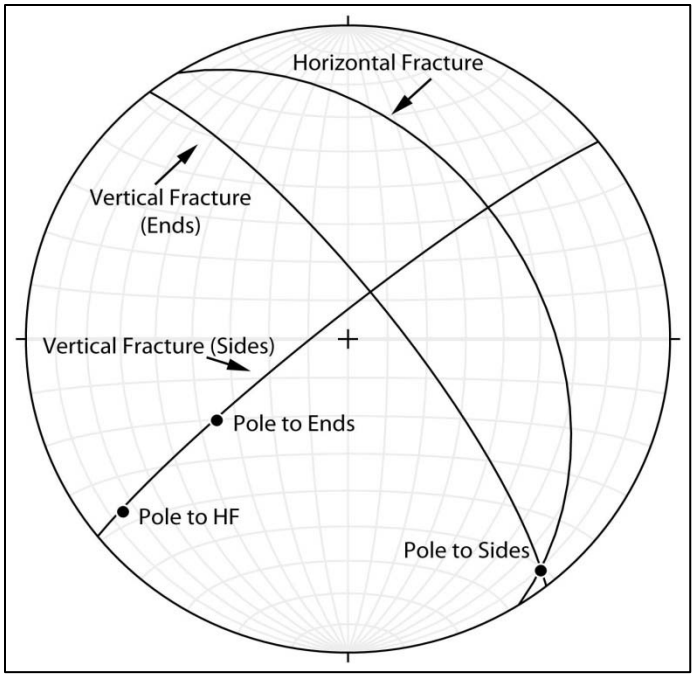

Figure 6. Stereonet representing the planes of fracturing within the quartzite headwall.

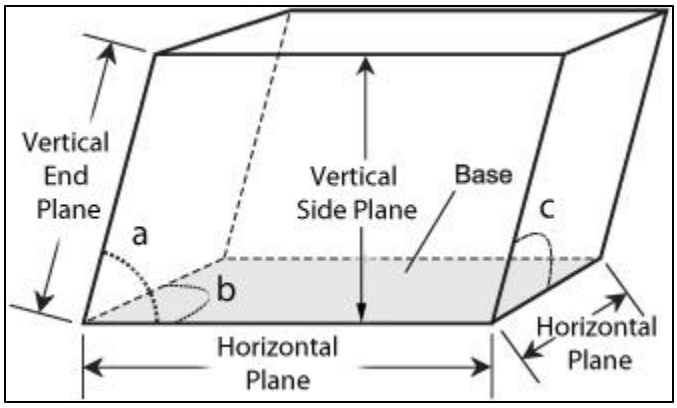

Figure 7. Block Diagram defining the relative location of each of the three planes of failure within the quartzite headwall.

Figure 8. South wall of cirque illustrating the bottom and sidewall failure planes (blue handled rock hammer for scale) Source: Greg Sedun

5.2 Lichenometry

Two separate pulses of rock fall activity are shown in the distribution of lichen thallus sizes (Figure 9). The cluster of lichen in size classes 25-44.9mm depicts a relatively long period of rock fall activity where new boulder surfaces were frequently being exposed for colonization. A smaller peak defined (approximately) by size classes 50-64.9mm portrays an earlier period of activity, as lichen sizes are larger but less frequent (i.e. older lichen are subject to greater risk of mortality). Size classes 45-49.9mm as well as classes smaller than 20-24.9mm indicate stagnant periods, as new rock surfaces were not exposed for lichen colonization at these times.

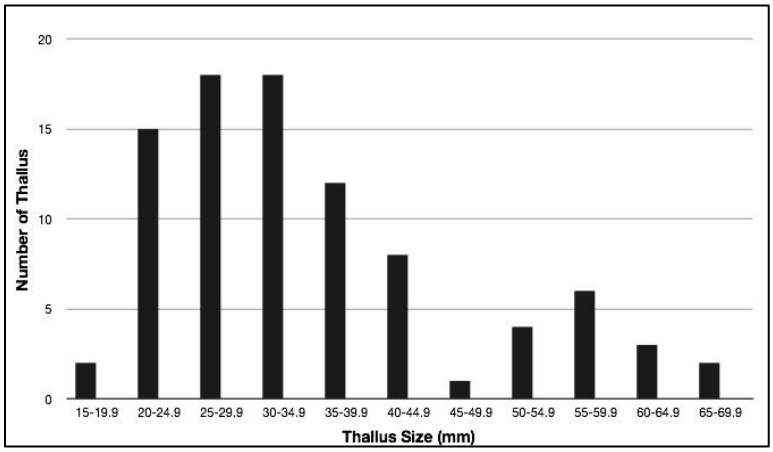

Figure 9. A frequency histogram illustrating the number of thalli measured in each 5-mm size class.

From 1770-1850, large boulders were released from the rockwall approximately every 25 years. The lichenometric survey (Figure 10) demonstrates a stagnant period of 20 years from 1850-1870 followed by an increased rate of large block failure to every 5 years over the next 50 years (1870-1910). Over the last 100 years however, large block failure appears to have ceased as no lichens were found to have diameters corresponding to dates after 1910. There was no correlation between spatial distribution and boulder ages observed from the lichenometric survey.

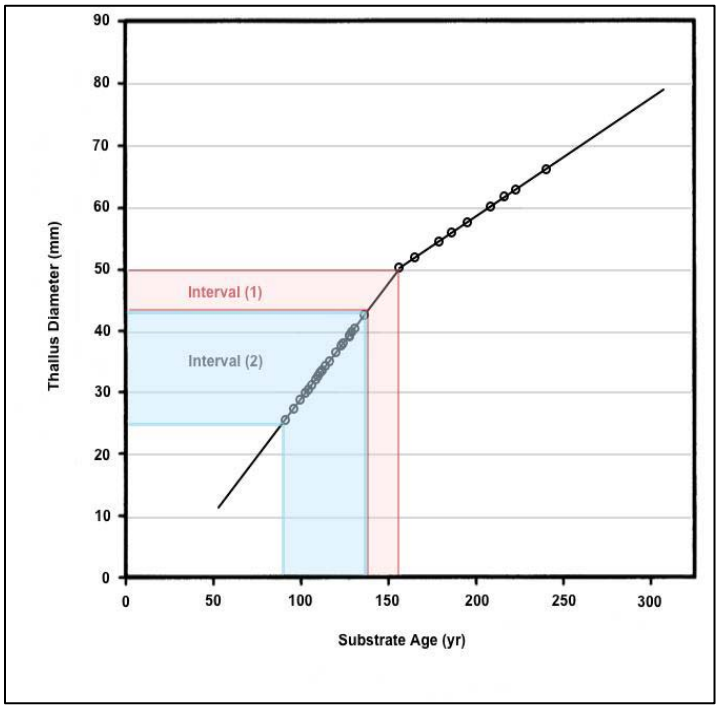

Figure 10. A lichen growth curve adapted from McCarthy (2003), which depicts the largest lichens within each sub-plot for the sampled Abbott Ridge cirque.

6. DISCUSSION

6.1 Structural interpretation of the headwall

As illustrated in Figure 6, the rock failure in the study site is characterized by three planes of fracturing. When these fractures are large enough they cause the ejection of a block from the cirque headwall. The horizontal fracture plane and the end wall vertical fracture plane intersect

in a line trending 141˚ with a plunge of 6˚, which happens to be the pole of the side vertical wall. Of large significance is similarity of the horizontal and end wall fracture planes to the Cheops fault with a strike of 320˚ (Geological Survey of Canada, 1962) and dipping towards to the northeast (Colpron et al. 1998). Perpendicular to both the horizontal and end wall fracture plane is the sidewall fracture plane. Each intersection of two planes is a potential for jointing and subsequent water entry.

Plate tectonics, prior geological stresses and glaciotectonics are the factors responsible for inducing stress into the cirque resulting in the previously mentioned fracture planes. The tectonic forces present in the formation of Abbott Ridge are responsible for the creation of the vertical end wall fracture plane. This is inferred through its similarity to the orientation of the Cheops fault. The horizontal and vertical sidewall fracturing are somewhat more complicated to explain. The most likely cause of the horizontal fracture plane is the failure along relict bedding planes from when the quartzite was sandstone. The degree to which glacial compression is involved in fracture formation is unknown, however the horizontal fracture plane does bear similarity to sheeting joints (McColl, 2012), a paraglacial feature.

The vertical sidewall fracture plane is most likely a culmination of multiple stresses from those involved with glaciotectonics to hydraulic forcing. The dip amount of the three failure planes provides a rough illustration for the shape of the rock fall debris and the large, angular boulders dated in this investigation indicate that joint spacing in the rockwall is conducive their failure.

6.2 Temporal indicators of rock fall frequency variability

Geomorphic processes at various time scales from micro to macro affect change in rock fall frequency. Generally, as the time scale increases, the magnitude of event also increases. These geomorphic processes are affected climatic and geological oscillations. Schumm & Lichty (1965) classify processes as falling into cyclic (10^6), graded (10^2) or steady (10^{-2}). Salient to this research are processes in the graded time scale, between 10^2 and 10^3 years. The graded time interval allows for a rough constraint on the processes that affect the rock fall frequency and remove scalar mismatches from consideration. The limitations of lichenometry, coupled with the

time allotted for data collection, limit the scale of analysis to events within 250 years; the scale of graded time.

Schumm and & Lichty (1965) propose that graded time scales are only dependent on responses to the system such as the hill slope morphology, drainage morphology and hydrology of a system. It is important to note that climatic variability influences graded time scales through factors such as increased hydrological activity and as a result the increased rate of rock fall frequency in the Abbott Ridge cirque (Wolman & Gerson, 1978). The dynamic behavior of the rockwall over the last 160 years indicates that external factors influencing failure rates fluctuated in magnitude and frequency, producing the observed response.

Preceding INTERVAL (1)

The period of 25-year failure frequency coincides with regional estimates of LIA pulses in the 18th and 19th centuries (Holm et al., 2004). Current occupation of the cirque by a small glacier infers the likelihood of glacial processes during this time. Glacial processes of erosion (i.e. plucking and abrasion) occur in conjunction with periglacial activity in the headwall to induce failure during this period (Seppälä, 2005).

INTERVAL (1)

Climate reconstructions of the Columbia Mountains indicate that a negative mass balance trend began around 1840 (Wood & Smith, in press.). Regional estimates of LIA terminal moraine dates also indicate that glacial response was triggered in the mid-19th century (Wilson & Luckman, 2002). This climatic transition is apparent in the rock fall frequency data obtained in this study. From 1850 to 1870, a lack of data suggests that large boulder failure was not occurring at the site. A lack of temperature data during this interval restricts the formation of climate-related comparisons; however, it is assumed that a period of climate warming was established around 1850. Parks Canada (2008) echoes this observation in their State of the Park report, indicating that overall glaciers in Glacier National Park have lost mass since 1850.

Permafrost degradation results from a thickening active layer; the increasing depth can occur immediately following deglaciation or develop with a slow temperature rise (Fischer, Kaab, Huggel, & Noetzli, 2006; Gruber & Haeberli, 2007). A lag time between permafrost

degradation, destabilization and subsequent failure is apparent in the dated talus, and explains the lack of rock fall events from 1850 to 1870. Further, paraglacial processes of debuttressing and stress release require glacial retreat, a process that may have been occurring during this 20-year time interval. As the glacier recedes towards the headwall, subsequent paraglacial processes begin, as is evident in the interval from 1870 to 1910.

INTERVAL (2)

From 1870 to 1910, increased rockfall frequency suggests two things:

(1) Paraglacial stress release and glacial debuttressing are influencing failure as glaciers retreat, uncovering compressed slopes and removing any stabilizing influence on the base of the rockwall. In order for a strong correlation between paraglacial processes and rockfall, dated talus deposits must indicate a high density of failures occurred soon after deglaciation (Cossart et al., 2008). As the deglaciation date of the Abbott Ridge cirque is unknown, it is only suggested that these mechanisms influenced failure rates around the time of retreat in the valley. Over this interval, an increase in the average seasonal temperatures during the winter months of 0.5˚ Celsius supports the deglaciation evidence; however, more information is required to attribute rockfall dynamics in the Abbott Ridge cirque to paraglacial origin.

(2) Climatically driven permafrost degradation may have triggered the high failure rates and rockfall frequency apparent after 1870. Measurements of rockwall temperature and permafrost indicators in the rockwall were not possible at the time of data collection however, based on the model proposed by Allen et al. (2009) we expect permafrost presence in the upper portion of the rockwall. The shaded headwall at Abbott Ridge is located in the marginal permafrost zone (~2000m), or the lower limit of discontinuous permafrost (Allen et al., 2009), where boulder detachment occurs (Kellerer-Pirklbauer et al., 2012). Interval (2) corresponds with the initiation of climatic warming in the surrounding area (Menounos et al., 2009) and this is supported by the rising trend in seasonal temperature averages for 2000m ASL in the study area. Permafrost response to warming temperatures is degradation. Recent studies indicate that warmer temperatures in high-mountain areas (3000m-3500m) are initiating permafrost degradation, triggering high frequency rock failure (Allen et al., 2009; Kellerer-Pirklbauer et al., 2012). Permafrost extent has migrated upwards since the last pulse of the LIA, and given the relatively

low altitude of the Abbott Ridge cirque headwall, it is suspected that permafrost degradation occurred from 1870 to 1910. Permafrost degradation is determined to be the major factor responsible for the observed increase in rockfall frequency over the second interval.

After INTERVAL (2)

From 1910 to present-day, the lichenometric samples indicate an absence of large boulder failure. Although there were no observations of lichen diameters in correspondence with rockfalls after 1910, the small sampling transect restricts our data set to those boulders located in the middle of the talus. This prevents a comprehensive estimate of current rates of rockwall failure. Further, since smaller rock sizes were not dated, it is unclear whether rockfalls of a different magnitude and frequency continue to occur; however, it is proposed that climatic warming has removed the majority of permafrost from the rockwall. In the Swiss Alps, permafrost degradation has encouraged very active failure, with rockfall rates stabilizing after its decimation (Kenner et al., 2011). In its absence, periglacial processes of seasonal freeze-thaw cycles, which operate on an annual basis, are responsible for weathering in the rockface (Matsuoka & Sakai, 1999). The current rate of rock failure is likely influenced by continued warming trends however the temporal scale of this relationship is of a finer resolution than lichenometry can capture.

Paraglacial causes should not be ruled out, however. The coarse data collection methods used in this study prevented the researchers from attributing the absence of rockfalls to the concept of paraglacial exhaustion. This tool has proven useful where an exponential decline in failure coincides with time elapsed since deglaciation. The model argues that there are a finite number of potential failure sites following deglaciation; locations of failure become ‘exhausted’ until paraglacial factors no longer influence rockfall frequency (Ballantyne, 2002). Cosmogenic isotope dating of talus surfaces has emerged as a promising method to test this concept; however, issues of time and money complicate its implementation (Cossart et al., 2008).

6.3 Sources of uncertainty

Several factors limited lichenometry as a method for dating/analyzing headwall retreat and slope-adjustment. Most importantly, there were some issues with accuracy, in both lichen

measurement and growth curve development. The process of lichen sampling comprised digital calipers of high precision, yet some uncertainty surrounded the accuracy of thallus measurements. Boulder surfaces were often uneven making it difficult to acquire accurate thallus measurements, reducing the accuracy of the caliper. Extensive snow coverage limited sampling methods to the selection of exposed surfaces. As such, the approach used in this research lacked the completeness of methods used by the lichenometric literature. Further, McCarthy's lichen growth curve for the neighboring Illecillewaet Glacier was adopted and modified to suit the needs of our investigation, ultimately offering a regional approximation of substrate age. This was the best growth curve available for the Abbott Ridge cirque, but it did not represent true substrate ages and thus might have caused error in our results.

A limited understanding of the sampled population's demographic history also restricted the analysis of growth patterns. For example, the shape of the histogram (which relates size and frequency of lichen thalli) is governed by rates of colonization and survival -- not individual growth rates (Loso & Doak, 2006). Older lichens have endured greater environmental stress (extreme weather, disease, etc.) and thus have higher mortality rates, making them increasingly rare within subplots (Loso & Doak, 2006). Consequently, the smaller size-frequency peaks associated with older lichens might have understated the magnitude of earlier rockfall activity.

Finally, the basic biological characteristics of lichen are not fully understood. This has contributed to scientific uncertainties surrounding the forces, which influence their colonization and survival rates (Bikerton & Matthews, 1992). In particular, an understanding of how lichen populations are affected by both local biological processes as well as climate change is currently limited (Luckman, 1977). The influence of these external forces on lichen growth patterns is unclear and likely affected our analysis in an immeasurable way.

Due to the lack of high resolution surface elevation data there is no method for determining quantitative data using Digital Elevation Model (DEM) morphometrics related to geomorphological processes such as surface creep, fluvial morphology, headwall retreat and topographical features. Further analysis of a DEM would have yielded valuable information used for deciphering features such as geological patterns, slope angle distributions and higher

order slope derivatives (Szekely & Karatson, 2004). There could have also been comparisons of a recent DEM to older elevation data from topographical maps.

7. CONCLUSION

7.1 Major findings

The major finding of this research is that surface dates in the center of the Abbott Ridge cirque talus indicate rockfall frequency increased after 1870. The factors responsible for this apparent increase occur over multiple timescales, from frequent frost weathering to climatic variability over 1000s of years. For the purposes of this investigation, only factors influencing rockfall variability over graded timescales (10^2) were considered, as permitted by the resolution of lichenometric surveys.

Terminal moraine building in the valley ceased at the time of increased rockfall frequency indicating that climatic warming evoked a response from periglacial and paraglacial processes responsible for triggering failure; however, their relative contributions remain unclear. Average seasonal temperatures after 1870 indicate a rising trend during winter months. Recent rockfall investigations underscore the influence of permafrost degradation as a triggering mechanism for elevated failure frequencies. This research proposes that permafrost degradation was active from 1870-1910 and triggered the high frequency failure rates observed in the Abbott Ridge cirque. Given the low elevation of the site, contemporary locations of permafrost likely only occur at the top of the ridge, if at all. This research indicates that permafrost degradation occurred coincidentally with glacial retreat in the area, contributing a temporally confined sediment source to mass movement processes in the valley system. Stabilization of headwall failure following permafrost degradation is consistent with the literature and is attributed to the removal of permafrost by rising air temperatures.

7.2 Directions for further research

To obtain an approximate deglaciation data, further research could date the Neoglacial moraine and the ancient moraine enclosing the cirque. Coupled with intensive lichenometric surveys along a cirque-normal transect this information could provide evidence for paraglacial

exhaustion. Paraglacial rock-slope evolution models indicate that failure frequency is highest following deglaciation, eventually slowing to a lesser frequency over time (Ballantyne, 2002). This relationship could be tested at the study site by establishing an inventory of mass movements and their timing based on numerous 14C dates. If the site reflected paraglacial exhaustion, results would indicate a distribution clustered around the deglaciation date. Given the scarcity of organic matter in alpine areas, another method to establish the deglaciation date as well as test for paraglacial exhaustion is to date surface exposure using cosmogenic isotope analysis (Cossart et al., 2008; Wilson, 2009).

Other potential research directions include deriving a headwall retreat rate. This could be accomplished by obtaining the total volume of total fallen rock, then using a combination of dendrochronology and lichenometry to get the amount of time that the headwall has been retreating. By getting an idea of the headwall retreat rate, a model of the head wall location through time could then be constructed (Matsuoka & Sakai, 1999). As well, it may reveal longer-term trends into how the headwall retreat rate varies with time. The headwall retreat rate could be used for a number of further studies including an investigation of glacier contact with the headwall. This headwall retreat rate could then be used to forecast when/if the headwall will continue to collapse all the way through Abbott Ridge. Also capable of predicting failure are further permafrost investigations. As contemporaneous results conclude, permafrost degradation is a major cause of rockfall activity. As the extent of permafrost migrates upwards, rockfall frequency measurements at incremental elevations on the face of surrounding peaks could provide insight into past events at Abbott Ridge as well as inform park management of slopes particularly susceptible to failure.

Acknowledgements

The authors would like to thank Dan Smith for facilitating the field component of this research and for his continued support through the writing process. The authors also appreciate the support from Bethany Coulthard, Jill Harvey, and Jessica Craig, both in the field and during report completion.

References

Allen, S. K., Gruber, S. and Owens, I.F. (2009). Exploring steep bedrock permafrost and its relationship with recent slope failures in the southern alps of new zealand. *Permafrost and Periglacial Processes, 20*(4), 345-356.

Allmendinger, R. W., Cardozo, N. C., and Fisher, D., 2012, Structural Geology Algorithms: Vectors & Tensors: Cambridge, England, Cambridge University Press, 289 pp.

Anastasiades, M., Brown, K., Byers, A., Fraser, K., Giuseppini, J., Neufeld, E., Pals, A., & Patterson, K. (2007). Mapping the retreat of the Asulkan glacier in Glacier National Park, British Columbia, Canada. Unpublished manuscript. Retrieved from http://www.geog.uvic.ca/dept2/faculty/smithd/geog477/paper2.pdf

Ballantyne, C.K. (2002). Paraglacial geomorphology. *Quaternary Science Reviews, 21*:1935-2017

Bikerton, R. W. & Matthews, J. A. (1992). On the accuracy of lichenometric dates: An assessment based on the 'Little Ice Age' moraine sequence of Nigardsbreen, southern Norway. *The Holocene, 2(227)*. DOI: 10.1177/095968369200200304

Colpron, M., Warren, M. J., & Price, R. A. (1998). Selkirk fan structure, southeastern canadian cordillera: Tectonic wedging against an inherited basement ramp. *Geological Society of America Bulletin, 110*(8), 1060-1074.

Compo, G.P., J.S. Whitaker, P.D. Sardeshmukh, N. Matsui, R.J. Allan, X. Yin, B.E. Gleason, R.S. Vose, G. Rutledge, P. Bessemoulin, S. Brönnimann, M. Brunet, R.I. Crouthamel, A.N. Grant, P.Y. Groisman, P.D. Jones, M. Kruk, A.C. Kruger, G.J. Marshall, M. Maugeri, H.Y. Mok, Ø. Nordli, T.F. Ross, R.M. Trigo, X.L. Wang, S.D. Woodruff, and S.J. Worley, 2011: The Twentieth Century Reanalysis Project. Quarterly J. Roy. Meteorol. Soc., 137, 1-28. DOI: 10.1002/qj.776

Cossart, E., Braucher, R., Fort, M., Bourlès, D. L., & Carcaillet, J. (2008). Slope instability in relation to glacial debuttressing in alpine areas (Upper Durance catchment, southeastern France): Evidence from field data and< sup> 10</sup> Be cosmic ray exposure ages. *Geomorphology*, *95*(1), 3-26.

Deline, P. (2009) Interactions between rock avalanches and glaciers in the Mont Blanc massif during the late Holocene. Quaternary Science Reviews, 28(11–12), 1070–1083 http://dx.doi.org/10.1016/j.quascirev.2008.09.025

Edelbro, C. 2003. *Rock Mass Strength: A Review*. Lulea University of Technology, Dept of Civil Engineering Division of Rock Mechanics.

Etzelmuller, B., Hoelzle, M., Heggem, E., Isaksen, K., Mittaz, C., Muhll, D., Odegard, R., Haeberli, W., & Sollid, J. (2001). Mapping and modelling the occurrence and distribution of mountain permafrost. Norsk Geografisk Tidsskrift - Norwegian Journal of Geography, 55(4): 186-194

Evans, I.S. (2006). Allometric development of glacial cirque form: Geological, relief, and regional effects on the cirques of Wales. *Geomorphology*, *80*:245-266

Fischer, L., Kaab, A., Huggel, C., & Noetzli, J. (2006). Geology, glacier changes, permafrost and related slope instabilities in a high-mountain rockwall: Monte Rosa east face, Italian Alps. *Natural Hazards and Earth Systems Science*, *6*: 761– 772.

French, H. M., & Slaymaker, O. (1993). *Canada's cold environments*. Montre□al: McGill-Queen's University Press.

Geertsema, M., Clague, J. J., Schwab, J. W., & Evans, S. G. (2006). An overview of recent large catastrophic landslides in northern British Columbia, Canada. *Engineering Geology*, *83*(1), 120-143.

Geological Survey of Canada. Rogers Pass[map]. 43-1962. 1:253,440. Ottawa, Canada: Department of Mines & Technical Surveys, 1962.

Google Inc (2012). Google Earth (Version 6.2) [Software]. Available from http://www.google.com/earth/download/ge/agree.html

Gruber S. & Haeberli, W. (2007). Permafrost in steep bedrock slopes and its temperature-related destabilization following climate change. Journal of Geophysical Research, *112*, F02S18, doi:10.1029/2006JF000547

Harrison, S., Anderson, E., & Patel, D. (2006). The eastern margin of glaciation in the British Isles during the Younger Dryas: The Bizzle cirque, southern Scotland. *Geografiska Annaler: Series A, Physical Geography*, *88*(3), 199-207.

Holm, K., Bovis, M., & Jakob, M. (2004). The landslide response of alpine basins to post-Little Ice Age glacial thinning and retreat in southwestern British Columbia. *Geomorphology*, *57*(3), 201-216.

Kellerer-Pirklbauer, A., Lieb, G.K., Avian, M., & Carrivick, J. (2012). Climate change and rock fall events in high mountain areas: numerous and extensive rock falls in 2007 at Mittlerer Burgstall, Central Austria. *Geografiska Annaler: Series A, Physical Geography*, DOI:10.1111/j.1468-0459.2011.00449.x

Kenner, R., Phillips, M., Danioth, C., Denier, C., Thee, P., & Zgraggen, A. (2011). Investigation of rock and ice loss in a recently deglaciated mountain rock wall using terrestrial laser scanning: Gemsstock, Swiss Alps. *Cold Regions Science and Technology, 67*(3):157–164

Loso, M. G. & Doak, D. F. (2006). The biology behind lichenometric dating curves. *Oecologia*, *147(2), pp. 223-229.* DOI: 10.1007/s00442-005-0265-3

Luckman, B. H. (1977). Lichenometric dating of holocene moraines at Mount Edith Cavell, Jasper, Alberta. *Canadian Journal of Earth Science, 14, pp. 1809-1822*. Retrieved from www.nrcresearchpress.com

Matsuoka, N. (2008). Frost weathering and rockwall erosion in the southeastern Swiss Alps: Long-term (1994-2006) observations. *Geomorphology, 99*: 353-368

Matsuoka, N., & Sakai, H. (1999). Rockfall activity from an alpine cliff during thawing periods. *Geomorphology, 28*(3–4), 309-328. doi: 10.1016/S0169-555X(98)00116-0

McCarthy, D. P. (2003). Estimating lichenometric ages by direct and indirect measurement of radial growth: A case study of Rhizocarpon agg. at the Illecillewaet Glacier, British Columbia. *Arctic, Antarctic, and Alpine Research, 35(2), pp. 203-213*. DOI: 10.1523-0430/0

McColl, S.T. (2012). Review: paraglacial rock-slope stability. *Geomorphology, 153-154*:1-16

Menounos, B., Osborn, G., Clague, J.J., & Luckman, B.H. (2009). Latest Pleistocene and Holocene glacier fluctuations in western Canada. *Quaternary Science Reviews, 28*(21-22): 2049-2074.

Mercier, D. (2009). Paraglacial and paraperiglacial landsystems: concepts, temporal scales and spatial distribution. *Géomorphologie: relief, processus, environnement*, (4/2008), 223-233.

Muller, G. (2006). On lichenometry and environmental history. *Environmental History, 11, pp. 604-609*. Retrieved from: http://envhis.oxfordjournals.org/content/11/3/604.full.pdf+html

Nelson, S.A. (2012). *Earthquakes and the Earth's interior.* [HTML] Retrieved from http://www.tulane.edu/~sanelson/eens1110/earthint.htm

Olyphant, G.A. (1981). Allometry and cirque evolution. *Geological Society of America Bulletin, Part 1, 92*:679-685

Parks Canada. (2008). Mount Revelstoke National Park of Canada and Glacier National Park of Canada: State of the Parks Report. Retrieved from http://www.pc.gc.ca/~/media/pn-np/bc/glacier/pdf/l-w/revglacSoPR_E.ashx

Parks Canada. (2012). Glacier National Park: The Columbia Mountains natural region. Retrieved from http://www.pc.gc.ca/eng/pn-np/bc/glacier/natcul/natcul1.aspx

Ravanel, L. & Deline, P. (2011). Climate influence on rockfalls in high-Alpine steep rockwalls: The north side of the Aiguilles de Chamonix (Mont Blanc massif) since the end of the 'Little Ice Age'. Holocene, 21(2): 357-365

Ritter, D. F., Kochel, R. C., & Miller, J. R. (2002). *Process Geomorphology*. Waveland Press, Inc.

Schumm, S. A., & Lichty, R. W. (1965). Time, space, and causality in geomorphology. *American Journal of Science, 263*(2), 110-119.

Seppälä, M. 2005. Session 3-Periglacial Landforms and Cryogenic Processes. *12 Late Contributions 219*, 55.

Slaymaker, O. (2011). Criteria to distinguish between periglacial, proglacial and paraglacial environments. *Quaestiones Geographicae 30(1), Bogucki Wydawnictwo Naukowe, Poznań, 9:*85–94

Szekely, B., & Karatson, D. (2004). DEM-based morphometry as a tool for reconstructing primary volcanic landforms: Examples from the Borzsony mountains, hungary. *Geomorphology, 63*(1), 25-37.

Taber, S. (1930). The mechanics of frost heaving. *The Journal of Geology, 38*(4), 303-317.

Watson, E. & Luckman, B.H. (2004). Tree-ring-based mass-balance estimates for the past 300 years at Peyto Glacier, Alberta, Canada. Quaternary Research, 62:9-18

Watson, E., & Luckman, B. H. (2004). Tree-ring-based mass-balance estimates for the past 300 years at Peyto Glacier, Alberta, Canada. *Quaternary Research, 62*(1), 9-18.

Wilson, P. (2009). Rockfall talus slopes and associated talus-foot features in the glaciated uplands of Great Britain and Ireland: periglacial, paraglacial or composite landforms? Geological Society Special Publications, 320:133-144

Wilson, R. J., & Luckman, B. H. (2002). Tree-ring reconstruction of maximum and minimum temperatures and the diurnal temperature range in British Columbia, Canada. *Dendrochronologia, 20*(3), 257-268.

Wolman, M. G., & Gerson, R. (1978). Relative scales of time and effectiveness of climate in watershed geomorphology. *Earth Surface Processes, 3*(2), 189-208.

Wood, L. & Smith, D. (In press). Climate and glacier mass balance trends from 1780 to present in the Columbia Mountains, British Columbia, Canada. *Holocene,* (accepted), 40p.

Worsley, P. (2007). Frost jacking of joint blocks above cwm idwal, in north wales. *Proceedings of the Geologists' Association, 118*(3), 277-281. doi: 10.1016/S0016-7878(07)80028-9

Zhu, T. 2012. *Some Useful Numbers on the Engineering Properties of Materials,* for Geology 615 at Stanford University, Department of Geophysics. Accessed October 24, 2012 from http://www.stanford.edu/~tyzhu/Documents/Some%20Useful%20Numbers.pdf

Further Readings

Aber, J.S., Croot, D.G. and Fenton, M.M. 1989. *Glaciotectonic landforms and structures*. Glaciology and Quaternary Geology Series, Kluwer Academic Publishers, Dordrecht, the Netherlands, 200 p.

Dobrowolski, R. (2009). Glaciotectonic deformations of the Upper Cretaceous rocks: evidence from the chalk quarry in Chełm (Lublin region, Eastern Poland). *Geologija*, *51*(3), 68-73.

Hicock, S. R., & Dreimanis, A. (1985). Glaciotectonic structures as useful ice-movement indicators in glacial deposits: four Canadian case studies. *Canadian Journal of Earth Sciences*, *22*(3), 339-346.

Nye, J. F. (1952). The mechanics of glacier flow. *J. Glaciol*, *2*(12), 82-93.

Sanders, J. W., Cuffey, K. M., MacGregor, K. R., Kavanaugh, J. L., & Dow, C. F. (2010). Dynamics of an alpine cirque glacier. *American Journal of Science*, *310*(8), 753-773.

Sharp, Martin. "Surging glaciers." *Progress in Physical geography* 12.4 (1988): 533-559.

Wheeler, J. O., 1963, Rogers Pass Map-Area, British Columbia and Alberta (82N W half): Geological Survey of Canada Paper 62-32, 32 p.

Whillans, I. M., & Veen, C. V. D. (1997). The role of lateral drag in the dynamics of Ice Stream B, Antarctica. *Journal of Glaciology-Only*, *43*(144), 231-237.

Zazoun, R. S., & Mahdjoub, Y. (2011). Strain analysis of Late Ordovician tectonic events in the In-Tahouite and Tamadjert Formations (Tassili-n-Ajjers area, Algeria). *Journal of African Earth Sciences*, *60*(3), 63-78.

APPENDIX A

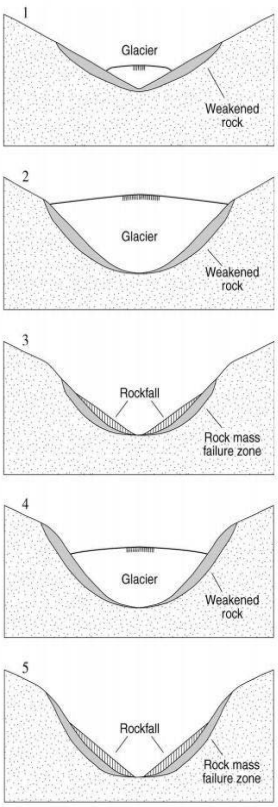

Figure 1. Paraglacial rockslope instability from glacial stress – from Ballantyne (2002).

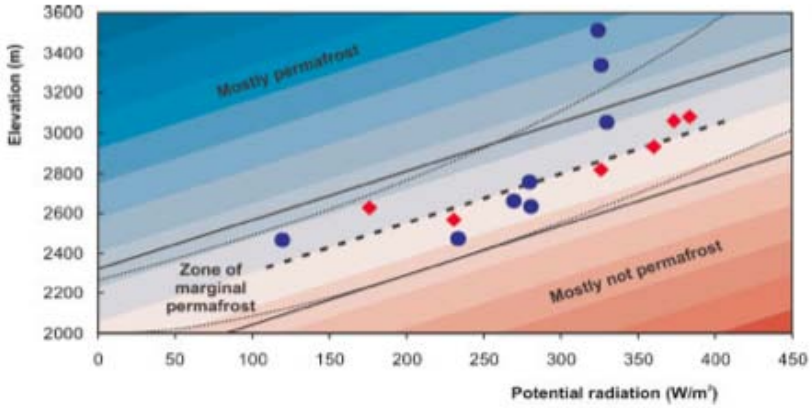

Figure 2. Classification of Permafrost Zones from Allen et al. (2009)